NOAA Technical Memorandum ERL WPL-76

METHOD TO CALCULATE PLUME PARAMETERS FROM SLANT ANGLE LIDAR DATA INCLUDING EFFECTS OF FINITE SPATIAL RESOLUTION

W. L. Eberhard

Wave Propagation Laboratory
Boulder, Colorado
July 1981

noaa NATIONAL OCEANIC AND ATMOSPHERIC ADMINISTRATION / Environmental Research Laboratories

NOAA Technical Memorandum ERL WPL-76

METHOD TO CALCULATE PLUME PARAMETERS FROM SLANT ANGLE LIDAR DATA INCLUDING EFFECTS OF FINITE SPATIAL RESOLUTION

W. L. Eberhard

Wave Propagation Laboratory
Boulder, Colorado
July 1981

UNITED STATES DEPARTMENT OF COMMERCE
Malcolm Baldrige, Secretary

NATIONAL OCEANIC AND ATMOSPHERIC ADMINISTRATION
John V. Byrne, Administrator

Environmental Research Laboratories
Joseph O. Fletcher, Acting Director

METHOD TO CALCULATE PLUME PARAMETERS FROM SLANT ANGLE LIDAR DATA INCLUDING EFFECTS OF FINITE SPATIAL RESOLUTION

Wynn L. Eberhard
NOAA/ERL/Wave Propagation Laboratory
Boulder, Colorado 80303

ABSTRACT

Lidars usually obtain plume profiles in planes oriented at angles slanted from a true cross section. These data can be projected onto a cross section to deduce parameters there such as the plume's burden, centroid, and dispersion coefficients. Except for the dispersion coefficients in some geometries, these three parameters can be calculated first in the slant section and converted to the equivalent cross-sectional forms. Some implications of the assumption made in projecting the data are considered. The lidar's finite spatial resolution causes a bias in the dispersion coefficient that can be removed by the method described.

INTRODUCTION

Lidar (or laser radar) has been shown to provide valuable information on particulate plume position and dispersion in air pollution and atmospheric flow studies. Early publications, such as those by Hamilton (1969) and Johnson and Uthe (1971), demonstrated the potential of the lidar. More recent work in this maturing field includes that of ground-based (Hoff and Froude, 1979) and airborne (Uthe, Nielsen, and Jimison, 1980) lidars. Increased utilization of lidar is anticipated as difficult problems are addressed regarding plume dynamics in complex terrain and in regimes of complicated stability and shear.

This paper discusses two interconnected characteristics of lidar data that can distort the inferred parameters of a plume unless the data are properly corrected for these effects. The first characteristic is that profiles of particulate concentrations are usually desired in cross sections normal to the plume's

centerline, but a lidar in most instances obtains data in planes or slant sections oriented at other angles. Even an airborne lidar, for which the direction of flight can be chosen, often for practical reasons gathers profiles in slant sections (Uthe, Nielsen, and Jimison, 1980). Plume parameters can be inferred by projecting the data onto the plane of the required cross section. This procedure is tantamount to assuming that the plume concentration in the locality of the slant section is invariant in the direction parallel to the centerline. Although this projection assumption is not true in the strict sense, the procedure is a reasonable method to determine some basic parameters. A similar challenge in data analysis is encountered by any sampling system not aligned in a cross section, including arrays of *in situ* samplers of plume constituents. Implications of the projection assumption are discussed further in the conclusions.

The second characteristic arises from the lidar's limited spatial resolution which can yield overestimates of plume dispersion coefficients, as shown below. This problem is also experienced by some other types of sensors, such as airborne *in situ* devices with limited response times. Corrections for this distortion in lidar data can be made which allow unbiased determination of plume dispersion even by lidars possessing poor spatial resolution, such as those with dye or CO_2 lasers with $\sim$100 m effective pulse lengths.

After a brief description of the attributes of lidar data, a coordinate system transformation to accomplish the projection is introduced. From the projected data the burden (here defined as the plume integrated lidar signal), centroid, and dispersion coefficients in the plume's cross section can be calculated. These parameters are compared with their counterparts in the slant section. The effects of the finite spatial resolution of the lidar on these parameters is also considered.

LIDAR DATA

Figure 1 is a diagram of a plume containing light-scattering particles undergoing sampling by a lidar scanning over a slanted plane. The X-axis is parallel to the plume's centerline, whose direction might be determined by any of several methods (Millan, 1976). Possible criteria include the direction of the mean wind

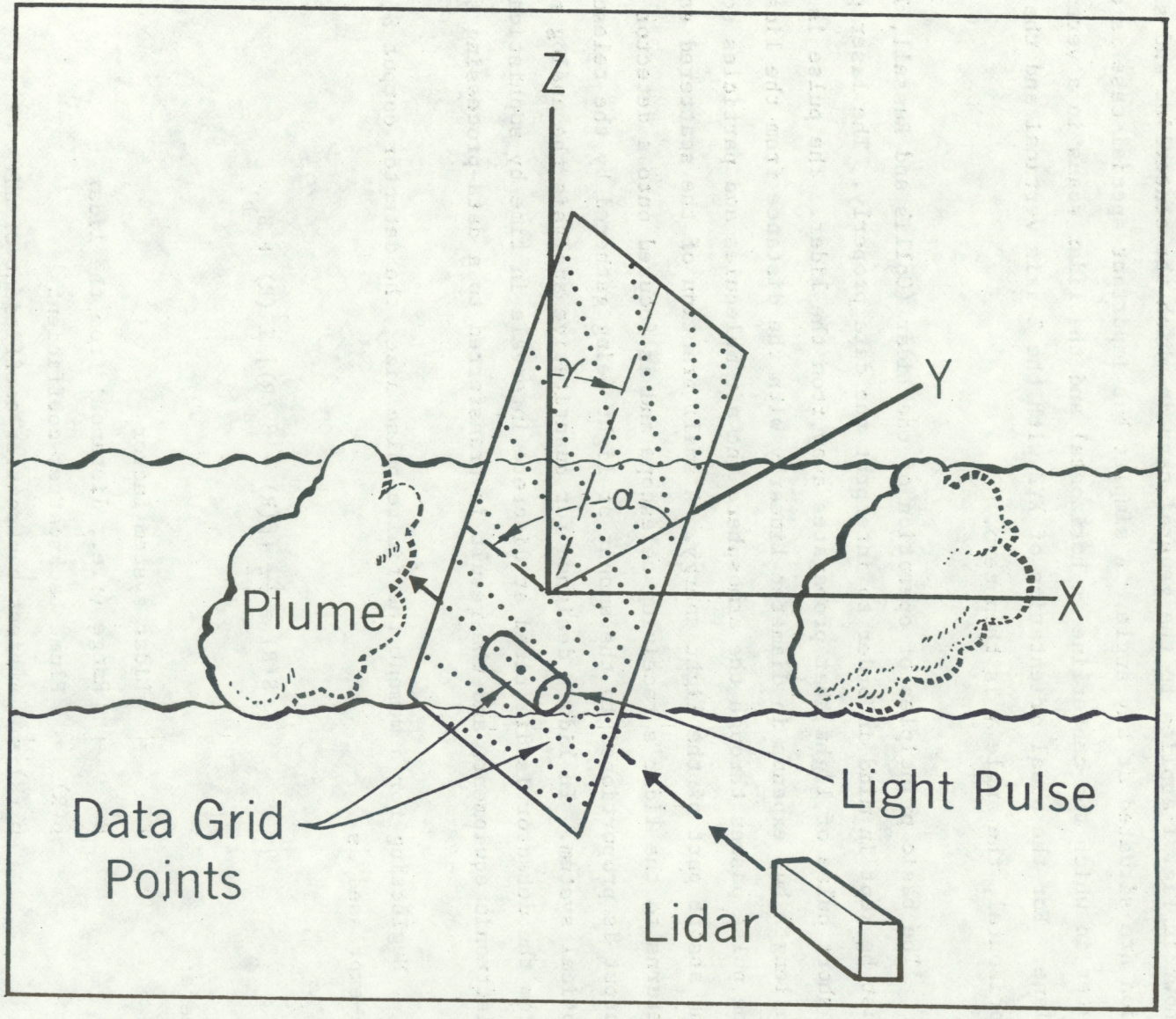

Figure 1.--Diagram of a lidar scanning a plume. The X-axis is parallel to plume centerline, and the Y-Z plane defines a plume cross section. The lidar scans a slant section which is skewed from the cross section by rotation angles α and γ.

measured nearby, a straight line between the source and the centroid of the lidar data, or a fit to a sequence of plume centroids as found by the lidar at several distances downwind. The lidar profile in the slant section will be projected onto the X = 0 plane to infer parameters in the plume's cross section. The geometry shown in Fig. 1 applies to the general case in which the centerline and slant section are situated at any angle. A simpler but important special case is discussed later in which the centerline is horizontal and the lidar scans in a vertical plane. For the usual orientation of XYZ with the Z-axis vertical and the Y-axis horizontal, the angle γ is then zero.

The basic principles of operation of the lidar (Collis and Russell, 1976) must be kept in mind in order to interpret the data properly. The laser produces a short pulse of light that propagates away from the lidar. The pulse is constant in length but expands in diameter linearly with the distance from the lidar. As the pulse passes through the atmosphere the air molecules and particles scatter and absorb part of the light energy. A small fraction of the scattered energy returns to the lidar's receiving telescope and is focused onto a detector whose output is proportional to the amount of light being gathered by the telescope's optical system. In lidars designed for quantitative analysis the analog signal from the detector is digitized at discrete intervals in time by sophisticated electronic equipment, and the result is transferred to a data-processing system.

Neglecting for a moment the finite pulse size, the detector output S(R) can be expressed as

$$S(R) = \frac{K}{R^2} [\beta(R) + \beta_a(R)] T^2(R) + S_b, \qquad (1)$$

where:

K	=	Lidar system factor
R	=	Range (i.e., distance) from the lidar
$\beta(R)$	=	Plume backscatter coefficient
$\beta_a(R)$	=	Ambient backscatter coefficient of air molecules plus natural aerosols
$T(R)$	=	One-way optical transmission over range R
S_b	=	Signal from background light and detector dark current.

The range is determined by

$$R = ct/2 \ , \tag{2}$$

where t is the elapsed time after pulse transmission and c is the speed of light. The factor of two accounts for the round-trip path of the scattered light. The backscatter coefficient at R is (in simple terms) the ratio of the energy scattered back toward the lidar to that laser energy incident on the atmosphere at R. Both the plume's particles and the molecules and natural aerosols of the ambient air contribute to the received signal via β and β_a respectively. The optical transmission T(R) accounts for the loss of energy in the pulse due to scattering and absorption.

The backscatter coefficients depend on several factors besides the number of scatterers. These other factors include the size distribution of the scatterers, their shape and composition, and the laser wavelength. If the particulates in the plume are constant in all these parameters except number density and multiple scattering is negligible, then β is directly proportional to the relative concentrations of the particles within the plume. We will here consider only profiles of β, leaving an examination of the constancy and interpretation of the optical characteristics of the scatterers to another forum.

In processing the data S(R) to obtain $\beta(R)$, corrections for S_b and R^2 are made first. Approximate corrections must also be made for optical transmission loss if significant. The contribution of β_a is removed by subtraction (or perhaps by applying a threshold if $\beta >> \beta_a$), which yields

$$\beta(R) = [S(R) - S_b] \frac{R^2}{K} T^{-2}(R) - \beta_a(R) \ . \tag{3}$$

This expression assumes an infinitesimal laser pulse size. For a finite pulse, and ignoring any small changes in R^2 and $T^2(R)$ over the extent of the pulse, the received signal at any instant is determined by the convolution of the three-dimensional pulse energy with the backscatter coefficient distribution. In order to state this mathematically, Fig. 2 shows a Cartesian coordinate system $\xi\eta\zeta$ traveling with the pulse, with the $x = 0$ and $\xi = 0$ planes congruent with the lidar scan plane. The effective energy density within the pulse with transmission loss

corrected is $I(\xi,\eta,\zeta)$. The term effective is used because of a factor of two compression in pulse length due to the round trip path of the scattered light (Collis and Russell, 1976) and elongation in signal in time from bandwidth limitations of the detector and electronic circuits. For simplicity, the energy density function is normalized according to

$$\int d\xi \int d\eta \int d\zeta \; I(\xi,\eta,\zeta) = 1 \; , \tag{4}$$

where the limits of integration are $-\infty$ to $+\infty$. The centroid is at the origin of $\xi\eta\zeta$, giving

$$\overline{\xi}_I = \int d\xi \int d\eta \int d\zeta \; \xi I(\xi,\eta,\zeta) = 0 \; , \tag{5}$$

with similar expressions for $\overline{\eta}_I$ and $\overline{\zeta}_I$. The lidar-measured value of backscatter coefficient β_L assigned to the point (x = 0, y, z) is therefore

$$\beta_L(0,y,z) = \int d\xi \int d\eta \int d\zeta \; I(\xi,\eta,\zeta)\beta(\xi,\; y+\eta,\; z+\zeta) \; . \tag{6}$$

If the pulse size is significant compared with features in the plume, the β_L profile will be a smeared version of the true β profile.

As mentioned earlier the lidar signal for each pulse is digitized at discrete intervals, which produces a series of data points along the line of propagation in the scan plane as indicated by one row of dots in Fig. 1. The lidar points at a slightly different angle for each successive pulse and builds up a two-dimensional data grid in the slant section. Inaccuracies, or discretization errors, which might occur in the β_L profile because the data are discrete rather than continuous, will be neglected here. If the grid is sufficiently dense, i.e., grid spacing is substantially smaller than plume features or pulse dimensions, the discretization error will be minor. Proper numerical analysis techniques (e.g., Hoff and Froude, 1979) must be utilized in processing the discrete data. In accord with the assumption of negligible discretization error and for the sake of simplicity the theoretical analysis pursued here will assume continuous data.

PROJECTION OF DATA

The method of projecting the lidar data from the slant section onto another plane to infer the plume's cross section will now be addressed. In Fig. 2 are shown four reference frames, each an orthogonal Cartesian system. XYZ might take any angular orientation but is shown in the geometry of the special case considered later.

In order to project the lidar data onto the cross-sectional plane X = 0, a transformation from xyz to XYZ coordinates is necessary. This is accomplished with the direction cosine matrix (Arfken, 1970)

$$\begin{bmatrix} X \\ Y \\ Z \end{bmatrix} = \begin{bmatrix} \hat{X}\cdot\hat{x} & \hat{X}\cdot\hat{y} & \hat{X}\cdot\hat{z} \\ \hat{Y}\cdot\hat{x} & \hat{Y}\cdot\hat{y} & \hat{Y}\cdot\hat{z} \\ \hat{Z}\cdot\hat{x} & \hat{Z}\cdot\hat{y} & \hat{Z}\cdot\hat{z} \end{bmatrix} \begin{bmatrix} x \\ y - y_o \\ z - z_o \end{bmatrix} , \tag{7}$$

where $\hat{X}\cdot\hat{x}$ is the vector dot product between the unit vectors parallel to the X and x axes, and so forth for the rest of the matrix elements. As a practical matter the unit vectors can be expressed in any single coordinate system, either one of those in Fig. 2 or another reference frame convenient in processing the data. The angle θ between the X and x axes, which is the same angle as exists between the X = 0 and x = 0 planes, is given in general by

$$\theta = \cos^{-1}(\hat{X}\cdot\hat{x}). \tag{8a}$$

For the special case shown in Fig. 2

$$\alpha = \theta . \tag{8b}$$

The projection transformation is developed from (7) by first recognizing that x = 0 because the lidar data are all in that plane. We next apply the projection assumption that $\beta(0,Y,Z) = \beta(X,Y,Z)$ for each point (X,Y,Z) in the slant section. The projection transformation is therefore given by

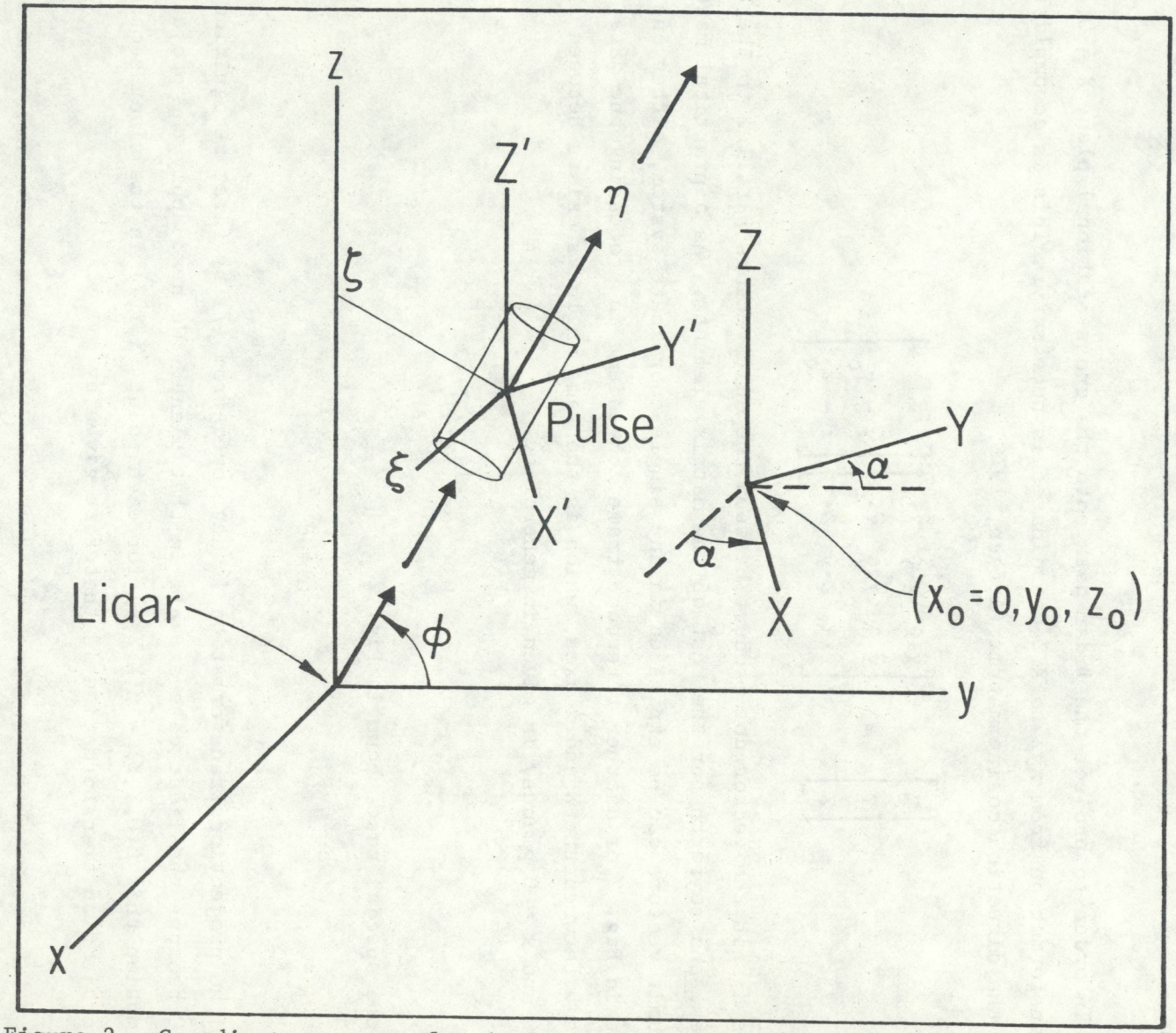

Figure 2.--Coordinate systems for derivations in the text. The lidar at the xyz origin scans in the x = 0 plane. $\xi\eta\zeta$ travels with the pulse in the η direction. XYZ is chosen with the X-axis parallel to plume centerline and origin in the lidar scan plane. X'Y'Z' has the same angular orientation as XYZ but with origin fixed to $\xi\eta\zeta$'s origin.

$$\begin{bmatrix} X = 0 \\ Y \\ Z \end{bmatrix} = \begin{bmatrix} 0 & 0 & 0 & 0 \\ \hat{Y}\cdot\hat{x} & \hat{Y}\cdot\hat{y} & \hat{Y}\cdot\hat{z} & y - y_o \\ \hat{Z}\cdot\hat{x} & \hat{Z}\cdot\hat{y} & \hat{Z}\cdot\hat{z} & z - z_o \end{bmatrix}. \tag{9}$$

The projected backscatter coefficient β_p from the lidar data is given by

$$\beta_p[0,Y,Z] = \beta_L[0,Y,Z] \tag{10a}$$

$$Y = (y-y_o)\ \hat{Y}\cdot\hat{y} + (z-z_o)\ \hat{Y}\cdot\hat{z} \tag{10b}$$

$$Z = (y-y_o)\ \hat{Z}\cdot\hat{y} + (z-z_o)\ \hat{Z}\cdot\hat{z}\ . \tag{10c}$$

This means that the value β_L measured by the lidar at $(x = 0,y,z)$ is projected onto the $X = 0$ plane at position (Y,Z) according to the relationships given in (10).

Needed in the discussion to follow is the projection $\beta_{po}(0,Y,Z)$ of the true backscatter coefficient $\beta(0,y,z)$ as would be measured by a lidar with an infinitesimally small pulse, namely

$$\beta_{po}[0,Y,Z] = \beta[0,y,z]\ . \tag{11}$$

PLUME PARAMETERS FROM PROJECTED DATA

Once the projection of the lidar data is completed the plume parameters sought in the cross section can be evaluated. Examined here are three parameters that are frequently needed, namely the integrated cross-sectional signal (or burden), the centroid, and the dispersion coefficients of the plume. The effect of the finite pulse size on each of these calculated from the projected lidar data is also examined.

The cross-sectional burden B is found by performing the integral

$$B = \int dY \int dZ\ \beta_p(0,Y,Z), \tag{12}$$

where the integrals are over all Y and Z with β_p set equal to zero where lidar data do not exist. The plume centroid in the cross section is located at

$$\bar{Y} = \frac{1}{B} \int dY \int dZ \; Y \; \beta_p(0,Y,Z) \; , \tag{13a}$$

$$\bar{Z} = \frac{1}{B} \int dY \int dZ \; Z \; \beta_p(0,Y,Z) \; . \tag{13b}$$

The dispersion coefficients σ_Y and σ_Z are defined by

$$\sigma_Y^2 = \frac{1}{B} \int dY \int dZ \; (Y-\bar{Y})^2 \; \beta_p(0,Y,Z) \tag{14a}$$

$$\sigma_Z^2 = \frac{1}{B} \int dY \int dZ \; (Z-\bar{Z})^2 \; \beta_p(0,Y,Z) \; . \tag{14b}$$

The effect of the finite pulse size can be determined by comparing the parameters in (12) through (14) calculated from the projected lidar data $\beta_p(0,Y,Z)$ with similar parameters (B_o, $\bar{Y}_o$, $\bar{Z}_o$, σ_{Yo}^2, and σ_{Zo}^2) calculated using the true projected profile of backscatter coefficients $\beta_{po}(0,Y,Z)$. In order to accomplish this the energy density function $I(\xi,\eta,\zeta)$ must be transformed to X'Y'Z' to give $I_p(X',Y',Z')$. The transformation matrix is

$$\begin{bmatrix} X' \\ Y' \\ Z' \end{bmatrix} = \begin{bmatrix} \hat{X}'\cdot\hat{\xi} & \hat{X}'\cdot\hat{\eta} & \hat{X}'\cdot\hat{\zeta} \\ \hat{Y}'\cdot\hat{\xi} & \hat{Y}'\cdot\hat{\eta} & \hat{Y}'\cdot\hat{\zeta} \\ \hat{Z}'\cdot\hat{\xi} & \hat{Z}'\cdot\hat{\eta} & \hat{Z}'\cdot\hat{\zeta} \end{bmatrix} \begin{bmatrix} \xi \\ \eta \\ \zeta \end{bmatrix} . \tag{15}$$

Since the total energy in the pulse is independent of the coordinate system that is chosen, we have

$$\int dX' \int dY' \int dZ' \; I_p(X',Y',Z') = 1 \; . \tag{16}$$

The position of the centroid within the pulse is also independent of the coordinate system. Since the centroid is at the common origin of $\xi\eta\zeta$ and X'Y'Z',

$$\bar{X}' = \bar{Y}' = \bar{Z}' = 0 \; . \tag{17}$$

Also needed are the pulse size coefficients given by

$$s_Y^2 = \int dX' \int dY' \int dZ' \; Y'^2 \; I_p(X',Y',Z') \tag{18a}$$

$$s_Z^2 = \int dX' \int dY' \int dZ' \; Z'^2 \; I_p(X',Y',Z') \; . \tag{18b}$$

In terms of the XYZ and X'Y'Z' coordinates, and by invoking the projection assumption that β is independent of X, the projected lidar data $\beta_p(0,Y,Z)$ are given by

$$\beta_p(0,Y,Z) = \int dX' \int dY' \int dZ' \; I_p(X',Y',Z')\beta(X',Y+Y',\; Z+Z'). \tag{19}$$

By substituting (19) into equations (12) through (14) the plume parameters from the projected lidar data β_p can be compared with the parameters of the true projected profile β_{po}.

In order to perform the integrals analytically we must assume that pulse diameter and angular orientation vary a negligible amount as the lidar scans through the plume. This condition is usually met unless the plume passes close to the lidar. In larger plumes the effects of finite pulse size diminish and the errors arising from the approximation are of little consequence.

Consider first the cross-sectional burden B, which can now be expressed as

$$B = \int dY \int dZ \int dX' \int dY' \int dZ' \; I_p(X',Y',Z')\beta(X',Y+Y',\; Z+Z').$$

Interchanging the order of integration and changing the variables of integration to

$$v = Y+Y' \tag{20a}$$

$$w = Z+Z' \tag{20b}$$

we have

$$B = \int dX' \int dY' \int dZ' \; I_p(X',Y',Z') \int dv \int dw \; \beta(X',v,w) \; .$$

Note that

$$\int dv \int dw \; \beta(X',v,w) = \int dY \int dZ \; \beta_{po}(0,Y,Z)$$

independent of X',Y', and Z'. Applying (16) gives the result

$$B = \int dY \int dZ \; \beta_{po}(0,Y,Z) = B_o \; . \tag{21}$$

The cross-sectional burden from the projected lidar data is therefore the same as that from the projected true backscatter coefficients and is unaffected by the finite pulse size.

A similar analysis for $\bar{Y}$ and $\bar{Z}$ shows that they also do not depend on finite pulse characteristics if the pulse's centroid is used to mark the pulse's position according to (5) and (17).

The plume variance, on the other hand, does depend on the characteristics of the finite pulse. For the Y-direction we have

$$\sigma_Y^2 = \frac{1}{B} \int dY (Y-\bar{Y})^2 \int dZ \int dX' \int dY' \int dZ' \; I_p(X',Y',Z') \beta(X',Y+Y',Z+Z') \; .$$

Application of (20) and changing the order of integration yields

$$\sigma_Y^2 = \frac{1}{B} \int dX' \int dY' \int dZ' \; I_p(X',Y',Z')$$

$$\times \int dv \int dw (v^2 + Y'^2 + \bar{Y}^2 - 2vY' - 2v\bar{Y} + 2Y'\bar{Y}) \beta(X',v,w) \; .$$

This reduces term-by-term to

$$\sigma_Y^2 = (\sigma_{Yo}^2 + \bar{Y}^2) + s_Y^2 + \bar{Y}^2 + 0 - 2\bar{Y}^2 + 0 = \sigma_{Yo}^2 + s_Y^2 \; . \tag{22a}$$

The result for the Z direction is

$$\sigma_Z^2 = \sigma_{Zo}^2 + s_Z^2 \; . \tag{22b}$$

The finite pulse size therefore causes an excessive estimate of plume dispersion.

The correct plume parameters B_o, $\bar{Y}_o$, and $\bar{Z}_o$ can be obtained directly from the projected lidar data. If s_Y^2 and s_Z^2 are known, the correct dispersions σ_{Yo}^2 and σ_{Zo}^2 can be calculated from the lidar data using (22).

PARAMETER CONVERSION (SPECIAL CASE)

In what is probably the most common experimental geometry the plume has a horizontal axis and is scanned by the lidar in vertical planes. This configuration is also noteworthy because simple formulas convert plume burden, centroid, and dispersion coefficients calculated in the slant section to those desired in the projected cross section. Mills, Allen and Butler (1978) and Hoff and Froude (1979) used these conversion factors in analysis of their data.

Figure 2 shows the necessary coordinate systems in which XYZ is formed by a rotation of the xyz system through angle α about the z axis and a translation to $(x_o = 0, y_o, z_o)$. The z and Z axes are both vertical, with the x,y,X, and Y axes horizontal. The projection matrix of the lidar data becomes

$$\begin{bmatrix} X \\ Y \\ Z \end{bmatrix} = \begin{bmatrix} 0 & 0 & 0 \\ -\sin\alpha & \cos\alpha & 0 \\ 0 & 0 & 1 \end{bmatrix} \begin{bmatrix} 0 \\ y - y_o \\ z - z_o \end{bmatrix} . \tag{23}$$

The projected lidar data are therefore given by (10a) where

$$Y = (y-y_o)\cos\alpha \tag{24a}$$

$$Z = z-z_o . \tag{24b}$$

The converse relationship is

$$\beta_L[0,y,z] = \beta_p[0,Y,Z] \tag{25a}$$

$$y = y_o + Y/\cos\alpha \tag{25b}$$

$$z = z_o + Z . \tag{25c}$$

The transformation matrix for the pulse energy density is

$$\begin{bmatrix} X' \\ Y' \\ Z' \end{bmatrix} = \begin{bmatrix} \cos\alpha & -\sin\alpha\cos\phi & -\sin\alpha\sin\phi \\ \sin\alpha & \cos\alpha\cos\phi & -\cos\alpha\sin\phi \\ 0 & \sin\phi & \cos\phi \end{bmatrix} \begin{bmatrix} \xi \\ \eta \\ \zeta \end{bmatrix} . \tag{26}$$

The plume parameters in the slant section will now be defined and compared to these in the cross section. The slant section burden is

$$b = \int dy \int dz \; \beta_L(0,y,z) \; . \tag{27}$$

The cross section burden from (12) can be expressed using (25) as

$$B = \int dY \int dZ \; \beta_L(0,y,z) \; .$$

Noting that

$$dY = dy \cos\alpha \tag{28a}$$

$$dZ = dz \; , \tag{28b}$$

we have the result in agreement with intuition that

$$B = \cos\alpha \int dy \int dz \; \beta_L(0,y,z) = b \cos\alpha \; . \tag{29}$$

The cross section burden is a factor $\cos\alpha$ smaller than the slant section burden because the area ratio of the portions of the two planes that intercept the plume is $\cos\alpha$.

The centroids can be evaluated in a similar manner. The expressions are

$$\bar{y} = \frac{1}{b} \int dy \int dz \;\; y \; \beta_L(0,y,z) \tag{30a}$$

$$\bar{z} = \frac{1}{b} \int dy \int dz \;\; z \; \beta_L(0,y,z) \; . \tag{30b}$$

The analogous factors in the cross section are

$$\bar{Y} = (\bar{y}-y_o)\cos\alpha \tag{31a}$$

$$\bar{Z} = \bar{z}-z_o \; . \tag{31b}$$

The spatial variances in the slant section are defined as

$$\sigma_y^2 = \frac{1}{b} \int dy \int dz \ (y-\bar{y})^2 \ \beta_L(0,y,z) \ , \tag{32a}$$

$$\sigma_z^2 = \frac{1}{b} \int dy \int dz \ (z-\bar{z})^2 \ \beta_L(0,y,z) \ . \tag{32b}$$

The conversion factors are determined to be

$$\sigma_Y^2 = \sigma_y^2 \cos^2\alpha \tag{33a}$$

$$\sigma_Z^2 = \sigma_z^2 \ . \tag{33b}$$

For the vertical slant section of a horizontal plume these cross-sectional plume parameters can be obtained by first calculating their analogs in the slant section and then applying simple correction factors. Since the amount of lidar data is voluminous, this procedure allows considerable economy and flexibility in data processing.

Determination of s_Y^2 and s_Z^2 for adjustment in σ_Y^2 and σ_Z^2 for finite resolution effects must be carried out in the same manner in both cases.

PARAMETER CONVERSION (GENERAL CASE)

Part of the results of the last section can be extended to the general case of arbitrary angular orientation of plume centerline and slant section.

Since the burden of a slant section and the projected cross section differ only by the ratio of the areas of the plume in each section, we have

$$B = b \cos\theta \ . \tag{34}$$

The projection relationship for the centroid can be determined by placing the origin of XYZ at the centroid in the slant section. For the special case just considered this results in $\bar{y} = y_o$, $\bar{z} = z_o$, and (31) becomes $\bar{Y} = \bar{Z} = 0$. The centroid of the projected data therefore coincides with the projection of the slant section's centroid. This is true for the general case as well, as can be

rigorously demonstrated by rotating xyz and XYZ while keeping the x = 0 and X = 0 planes constant in such a way that the mathematics of the special case apply. The positions of the slant section and cross section centroids are not changed by such rotations, and the same conclusion is reached as in the special case. For the projection transformation given in (9) we therefore have

$$\bar{Y} = (\bar{y}-y_o)\hat{Y}\cdot\hat{y} + (\bar{z}-z_o)\hat{Y}\cdot\hat{z} \tag{35a}$$

$$\bar{Z} = (\bar{y}-y_o)\hat{Z}\cdot\hat{y} + (\bar{z}-z_o)\hat{Z}\cdot\hat{z} \quad . \tag{35b}$$

It is impossible to handle the dispersion coefficients in such a convenient manner. The reason is that the projections of the y and z axes onto the X = 0 plane are not orthogonal. This prevents expression of σ_Y^2 and σ_Z^2 in terms of σ_y^2 and σ_z^2 unless rigid assumptions about plume symmetry can be made that are rarely realized in nature. Unlike the special case the dispersion coefficients in the general case can be computed only by first projecting the lidar data onto the cross-sectional plane.

CONCLUSIONS

This treatment of the projection of lidar data onto a plume's cross-sectional plane in order to infer parameters there has involved three topics: 1) the validity of the projection assumption; 2) relationships governing the conversion of plume burden, centroid, and dispersion coefficients from a slant section to the cross section; and 3) corrections for bias in the dispersion coefficients when the lidar pulse size is not negligible compared with the plume's transverse dimensions. Both the general case and the special case of a vertical slant section of a horizontal plume were considered.

The implications of projecting the slant section lidar data onto a cross-sectional plane must be carefully considered before interpreting the data in any specific manner. Putting aside for the moment any plume expansion with distance downwind, turbulent mixing causes random fluctuations in concentration along the plume. These fluctuations create statistical variations in measurements of burden, centroid, and dispersion coefficients, even when made in a true cross section. It

is reasonable to consider the projection assumption to be valid in deducing these three parameters from slant section data if typical or average (over repeated scans) values are sought. An example where the assumption is not valid is in the determination of the spatial spectrum of inhomogeneities in the plume's concentration through a cross section. The variations along the plume would shift the spatial spectrum of projected data to higher spatial frequencies. Slant section data in such an application are not necessarily useless, for it might be possible to devise a method to correct the bias.

The analysis of the effects of finite lidar resolution also incorporated the projection assumption. Although inhomogeneities along the plume can alter any individual experimental measurement, the analysis is believed to be proper in the typical or average sense.

Millan (1976) considered some aspects of interpreting projected data when a plume widens appreciably over the extent of a slant section. If the lidar measures the dispersion coefficients at several distances downwind, it should be possible to determine the approximate rate of dispersion and correct to a reasonable extent the errors due to the slant section.

A coordinate system transformation to project the lidar data in a slant section onto a cross-sectional plane was described. The burden and centroid of the plume can be computed from the projected data, or they can first be calculated in the slant section and accurately converted to their cross-sectional equivalent. A similar procedure can be followed to deduce the dispersion coefficient in the special case of a vertical slant section of a horizontal plume. In the general case the cross-sectional dispersion coefficients can be properly calculated only after projecting the lidar data onto the cross section.

The finite resolution of the lidar does not alter the values determined for the burden or position of the centroid. It does cause an excessive estimate of the dispersion coefficients, but a correction can be applied by projecting the three-dimensional distribution of pulse energy density into the plume-oriented XYZ coordinate system to find the pulse's size coefficients.

Financial support for this research was provided by the U.S. Environmental Protection Agency under the EPA-NOAA Interagency Energy/Environment Agreement.

REFERENCES

1. Arfken G. (1970) Mathematical Methods for Physicists. Academic Press.

2. Collis R.T.H. and Russell P.B. (1976) Lidar measurement of particles and gases by elastic scattering and differential absorption. In Topics in Applied Physics, 14, Hinkley E.D., ed. Springer-Verlag.

3. Hamilton P.M. (1969) The application of a pulsed-light rangefinder (lidar) to the study of chimney plumes. Phil. Trans. Roy. Soc. Lond., A265, 153-172.

4. Hoff R.M. and Froude F.A. (1979) Lidar observation of plume dispersion in northern Alberta. Atmospheric Environment, 13, 35-43.

5. Johnson W.B. and Uthe E.E. (1971) Lidar study of the Keystone stack plume. Atmospheric Environment, 5, 703-724.

6. Millan M.M. (1976) A note on the geometry of plume diffusion measurements. Atmospheric Environment, 10, 655-658.

7. Mills F.S., Allen R.J. and Butler C.F. (1978) An experimental/analytical program to assess the utility of lidar for pollution monitoring. Dept. Physics and Geophysical Sciences, Old Dominion Univ. Tech. Rpt. PGSTR-AP78-9, Norfolk, VA., U.S.A.

8. Uthe E.E., Nielsen N.B. and Jimison W.L. (1980) Airborne lidar plume and haze analyzer (ALPHA-1). Bull. Amer. Meteor. Soc., 61, 1035-1043.